

# Axial Collective Mode of a Dipolar Quantum Droplet

Peter Blair Blakie 

Department of Physics and Dodd-Walls Centre for Photonic and Quantum Technologies, University of Otago, Dunedin 9016, New Zealand; blair.blakie@otago.ac.nz

**Abstract:** In this work, we investigate the ground state properties and collective excitations of a dipolar Bose–Einstein condensate that self-binds into a quantum droplet, stabilized by quantum fluctuations. We demonstrate that a sum rule approach can accurately determine the frequency of the low energy axial excitation, using properties of the droplet obtained from the ground state solutions. This excitation corresponds to an oscillation in the length of the filament-shaped droplet. Additionally, we evaluate the static polarizabilities, which quantify change in the droplet dimensions in response to a change in harmonic confinement.

**Keywords:** dipolar Bose–Einstein condensate; quantum droplets; collective excitations

## 1. Introduction

A dipolar Bose–Einstein condensate (BEC) is made up of particles with a significant dipole moment, making dipole–dipole interactions (DDIs) important. Highly magnetic atoms have been used in experiments to create dipolar BECs [1–4] and to explore various phenomena arising from these interactions [5,6]. In the dipole-dominated regime, where DDIs dominate over short-ranged interactions, quantum droplets can be formed. These droplets are mechanically unstable at the mean-field level, but are stabilized against collapse by quantum fluctuations [7–13]. Experiments using dysprosium [11,14,15] and erbium [16] atoms have prepared and measured various properties of these quantum droplets, which have a filament-like shape due to the anisotropy of the DDIs.

The extended Gross–Pitaevskii equation (EGPE) provides a theoretical description of the ground states and dynamics of quantum droplets, incorporating quantum fluctuation effects within a local density approximation. The collective excitations of these quantum droplets are described by the Bogoliubov–de Gennes (BdG) equations, which can be obtained by linearizing the time-dependent EGPE about a ground state. Baillie et al. [17] presented the results of numerical calculations of the collective excitations of a dipolar quantum droplet (also see [18]). Additionally, a class of three shape excitations has been approximated using a Gaussian variational ansatz [19]. Experiments have measured the lowest energy shape excitation, corresponding to the lowest nontrivial axial mode, for a large trapped droplet [16]. Experiments with dysprosium droplets have also measured the scissors mode [20].

In this paper, we consider dipolar quantum droplet ground states and the  $m = 0$  (projection of angular momentum quantum number) collective excitations in free-space cases and in trapped cases. We focus on a low energy axial collective excitation, which softens to zero energy to reveal the unbinding (evaporation) point for a free-space quantum droplet. We use a sum rule approach to estimate the excitation frequency of this mode in terms of the ground state properties, including its static response to a small change in the axial trapping frequency. We compare the result of this sum rule method to the excitation frequency obtained by direct numerical solution of the BdG equations. We verify that the sum rule predictions are accurate over a wide parameter regime, including deeply bound droplet states, droplets close to the unbinding threshold, and in the trapped situation where the droplet crosses over to a trap-bound BEC.



**Citation:** Blakie, P.B. Axial Collective Mode of a Dipolar Quantum Droplet. *Photonics* **2023**, *10*, 393. <https://doi.org/10.3390/photonics10040393>

Received: 10 March 2023

Revised: 31 March 2023

Accepted: 31 March 2023

Published: 1 April 2023



**Copyright:** © 2023 by the author. Licensee MDPI, Basel, Switzerland. This article is an open access article distributed under the terms and conditions of the Creative Commons Attribution (CC BY) license (<https://creativecommons.org/licenses/by/4.0/>).

## 2. Formalism

### 2.1. Ground States

Here we consider a gas of magnetic bosonic atoms described by the EGPE energy functional

$$E = \int d\mathbf{x} \psi^* \left[ h_{\text{sp}} + \frac{1}{2} g_s |\psi|^2 + \frac{1}{2} \Phi_{\text{dd}} + \frac{2}{5} \gamma_{\text{QF}} |\psi|^3 \right] \psi, \quad (1)$$

where

$$h_{\text{sp}} = -\frac{\hbar^2}{2M} \nabla^2 + V(\mathbf{x}), \quad (2)$$

$$V(\mathbf{x}) = \frac{1}{2} M (\omega_x^2 x^2 + \omega_y^2 y^2 + \omega_z^2 z^2), \quad (3)$$

are the single particle Hamiltonian and the harmonic trapping potential, respectively. Here,  $g_s = 4\pi\hbar^2 a_s / M$  is the coupling constant for the contact interactions, where  $a_s$  is the  $s$ -wave scattering length. The potential

$$\Phi_{\text{dd}}(\mathbf{x}) = \int d\mathbf{x}' U_{\text{dd}}(\mathbf{x} - \mathbf{x}') |\psi(\mathbf{x}')|^2, \quad (4)$$

describes the long-ranged DDIs, where the magnetic moments of the atoms are polarized along  $z$  with

$$U_{\text{dd}}(\mathbf{r}) = \frac{3g_{\text{dd}}}{4\pi r^3} \left( 1 - \frac{3z^2}{r^2} \right). \quad (5)$$

Here  $g_{\text{dd}} = 4\pi\hbar^2 a_{\text{dd}} / M$  is the DDI coupling constant, with  $a_{\text{dd}} = M\mu_0\mu_m^2 / 12\pi\hbar^2$  being the dipolar length, and  $\mu_m$  the atomic magnetic moment. The quantum fluctuations are described by the nonlinear term with coefficient  $\gamma_{\text{QF}} = \frac{32}{3} g_s \sqrt{a_s^3} / \pi Q_5(\epsilon_{\text{dd}})$ , where

$$Q_5(x) = \Re \left\{ \int_0^1 du [1 + x(3u^2 - 1)]^{5/2} \right\}, \quad (6)$$

(see reference [8]) and  $\epsilon_{\text{dd}} \equiv a_{\text{dd}} / a_s$ . We constrain solutions to have a fixed number of particles  $N$  and ground state solutions satisfy the EGPE

$$\mu\psi = \mathcal{L}_{\text{EGP}}\psi, \quad (7)$$

where  $\mu$  is the chemical potential and we introduced

$$\mathcal{L}_{\text{EGP}}\psi = \left( h_{\text{sp}} + g_s |\psi|^2 + \Phi_{\text{dd}} + \gamma_{\text{QF}} |\psi|^3 \right) \psi. \quad (8)$$

For the results we present here we leveraged the algorithm developed in Reference [21] to calculate the ground states.

### 2.2. Excitations

#### 2.2.1. Bogoliubov–De Gennes Theory

The collective excitations are described within the framework of Bogoliubov theory. These excitations can be obtained by linearizing the time-dependent EGPE  $i\hbar\dot{\Psi} = \mathcal{L}_{\text{EGP}}\Psi$  around a ground state using an expansion of the form

$$\Psi(\mathbf{x}, t) = e^{-i\mu t} \left[ \psi(\mathbf{x}) + \sum_{\nu} \left\{ \lambda_{\nu} u_{\nu}(\mathbf{x}) e^{-i\omega_{\nu} t} - \lambda_{\nu}^* v_{\nu}^*(\mathbf{x}) e^{i\omega_{\nu} t} \right\} \right], \quad (9)$$

where  $\lambda_\nu$  are the (small) expansion coefficients. The excitation modes  $u_\nu, v_\nu$  and frequencies  $\omega_\nu$  satisfy the BdG equations

$$\begin{pmatrix} \mathcal{L}_{\text{EGP}} - \mu + X & -X \\ X & -(\mathcal{L}_{\text{EGP}} - \mu + X) \end{pmatrix} \begin{pmatrix} u_\nu \\ v_\nu \end{pmatrix} = \hbar\omega_\nu \begin{pmatrix} u_\nu \\ v_\nu \end{pmatrix}, \tag{10}$$

where  $X$  is the exchange operator given by

$$Xf \equiv g_s |\psi_0|^2 f + \psi_0 \int d\mathbf{x}' U_{\text{dd}}(\mathbf{x} - \mathbf{x}') f(\mathbf{x}') \psi_0^*(\mathbf{x}') + \frac{3}{2} \gamma_{\text{QF}} |\psi_0|^3 f. \tag{11}$$

More details of the Bogoliubov analysis of the EGPE can be found in Reference [17]. Here we consider problems with rotational symmetry about the  $z$  axis, which restricts the trap to cases with  $\omega_x = \omega_y$ . This symmetry means that the excitations can be chosen to have a well-defined  $z$ -component of angular momentum,  $\hbar m$ , where we introduced  $m = 0, \pm 1, \pm 2, \dots$  as the quantum number.

### 2.2.2. Sum Rule Approach for Lowest Compressional Mode

We now wish to discuss a method for extracting the low energy axial compressional mode. We consider the mode excited by the axial operator  $\sigma_z = \int d\mathbf{x} \hat{\psi}^\dagger z^2 \hat{\psi}$ , where  $\hat{\psi}$  is the bosonic quantum field operator. The energy ( $\hbar\omega_{\text{ub}}$ ) of the lowest mode excited by  $\sigma_z$  has an upper bound provided by the ratio  $\sqrt{m_1/m_{-1}}$ , where we introduced  $m_p = \int d\omega (\hbar\omega)^p S_z(\omega)$  as the  $p$ -moment of  $S_z(\omega)$  [22]. Here

$$S_z(\omega) = \hbar \sum_p |\langle p | \sigma_z | 0 \rangle|^2 \delta(E_p - E_0 - \hbar\omega), \tag{12}$$

is the zero temperature dynamic structure factor, with  $|p\rangle$  being the eigenstate of the second quantized Hamiltonian  $H$  of energy  $E_p$ , and  $|0\rangle$  denotes the ground state. The  $m_1$  moment can be evaluated using a commutation relation as

$$m_1 = \frac{1}{2} \langle 0 | [\sigma_z, [H, \sigma_z]] | 0 \rangle = \frac{2N\hbar^2 \langle z^2 \rangle}{M}. \tag{13}$$

The  $m_{-1}$  moment can be evaluated as  $m_{-1} = \frac{1}{2} \chi_{zz}$  (see [22]), where  $\chi_{zz}$  is the static polarizability quantifying the linear response of  $\sigma_z$  to the application of the perturbation  $-\lambda\sigma_z$  to the Hamiltonian, i.e.,  $\delta\langle\sigma_z\rangle = \lambda\chi_{zz}$ . Setting  $\lambda \equiv -\frac{1}{2}M\delta\omega_z^2$ , we see that this perturbation is equivalent to a change in the axial trapping frequency, and, hence, the static polarizability can be evaluated as

$$\chi_{zz} = -\frac{2N\delta\langle z^2 \rangle}{M\delta\omega_z^2}, \tag{14}$$

(the reader can also see References [22–24]). Thus, we obtain the following as an upper-bound estimate of the lowest mode frequency

$$\omega_{\text{ub}} = \sqrt{\frac{4N\langle z^2 \rangle}{M\chi_{zz}}}. \tag{15}$$

A similar approach was used in Reference [20] to estimate the scissors mode frequency of a dipolar droplet, but in that work the  $z$ -component of angular momentum was the relevant excitation operator.

It is also of interest to understand the static polarizability quantifying the change in the transverse width (with operator  $\sigma_\rho = \int d\mathbf{x} \hat{\psi}^\dagger \rho^2 \hat{\psi}$ , where  $\rho = \sqrt{x^2 + y^2}$ ) to the axial perturbation, i.e.,

$$\chi_{\rho z} = -\frac{2N\delta\langle\rho^2\rangle}{M\delta\omega_z^2}. \tag{16}$$

Later, we consider both the *axial*  $\chi_{zz}$  and *transverse*  $\chi_{\rho z}$  static polarizabilities to characterize quantum droplet behavior.

### 3. Results for Free-Space Droplets

#### 3.1. Energetics

In Figure 1 we consider a free-space (self-bound)  $^{164}\text{Dy}$  droplet for  $a_s = 80 a_0$  (i.e.,  $\epsilon_{\text{dd}} = 1.64$ ) as a function of  $N$ . For  $N > N_{\text{crit}} \approx 2020$  a self-bound droplet solution exists while, for  $N < N_{\text{crit}}$ , there is no droplet solution, and the atoms expand to fill all space. This value of  $N_{\text{crit}}$  is slightly higher than the value obtained in Reference [17] for the same physical parameters. This is because we use the result  $Q_5(\epsilon_{\text{dd}})$ , rather than the approximation  $1 + \frac{3}{2}\epsilon_{\text{dd}}^2$ , to define  $\gamma_{\text{QF}}$ .

In Figure 1a we examine the energy of the free-space droplet, and observe that, as  $N$  approaches  $N_{\text{crit}}$  from above, the total energy of the droplet becomes positive (for  $N \lesssim 2350$ , see inset). When the energy is positive the droplet is metastable. We show some examples of the droplet states in Figure 1c to give some context on the size and shape of the droplet as  $N$  varies.

We also consider the components of energy, defined by

$$E_{\text{kin}} = -\frac{\hbar^2}{2M} \int d\mathbf{x} \psi^* \nabla^2 \psi, \tag{17}$$

$$E_{\text{pot}} = \int d\mathbf{x} V(\mathbf{x}) |\psi|^2, \tag{18}$$

$$E_s = \frac{1}{2} g_s \int d\mathbf{x} |\psi|^4, \tag{19}$$

$$E_{\text{dd}} = \frac{1}{2} \int d\mathbf{x} \Phi_{\text{dd}}(\mathbf{x}) |\psi|^2, \tag{20}$$

$$E_{\text{QF}} = \frac{2}{5} \gamma_{\text{QF}} \int d\mathbf{x} |\psi|^5 \tag{21}$$

as the kinetic, potential, contact interaction, DDI, and quantum fluctuation energy, respectively. For this free-space case  $E_{\text{pot}} = 0$ , and we observe that the DDI and contact interaction energies are the largest energies by magnitude, but have opposite signs. The quantum fluctuation term is necessary to stabilize the droplet solution against mechanical collapse driven by the interaction terms, but is typically significantly smaller in magnitude than either of the interaction energies. The kinetic energy is smaller than all other components, except when  $N \rightarrow N_{\text{crit}}$ , where it can exceed  $E_{\text{QF}}$ .

A virial relation for the system can be obtained by considering how the energy functional transforms under a scaling of coordinates (e.g., see [25]). For the dipolar EGPE in a harmonic trap this relation is

$$\Lambda \equiv E_{\text{kin}} - E_{\text{pot}} + \frac{3}{2}(E_s + E_{\text{dd}}) + \frac{9}{4}E_{\text{QF}} = 0, \tag{22}$$

and provides a connection between the energy components [21,26]. In Figure 1a we show  $\Lambda$  for reference. This turns out to be a sensitive test of the accuracy of dipolar quantum droplet solutions [21], and the results we present here typically have  $|\Lambda/N\hbar| \ll 10^{-3}$  Hz.

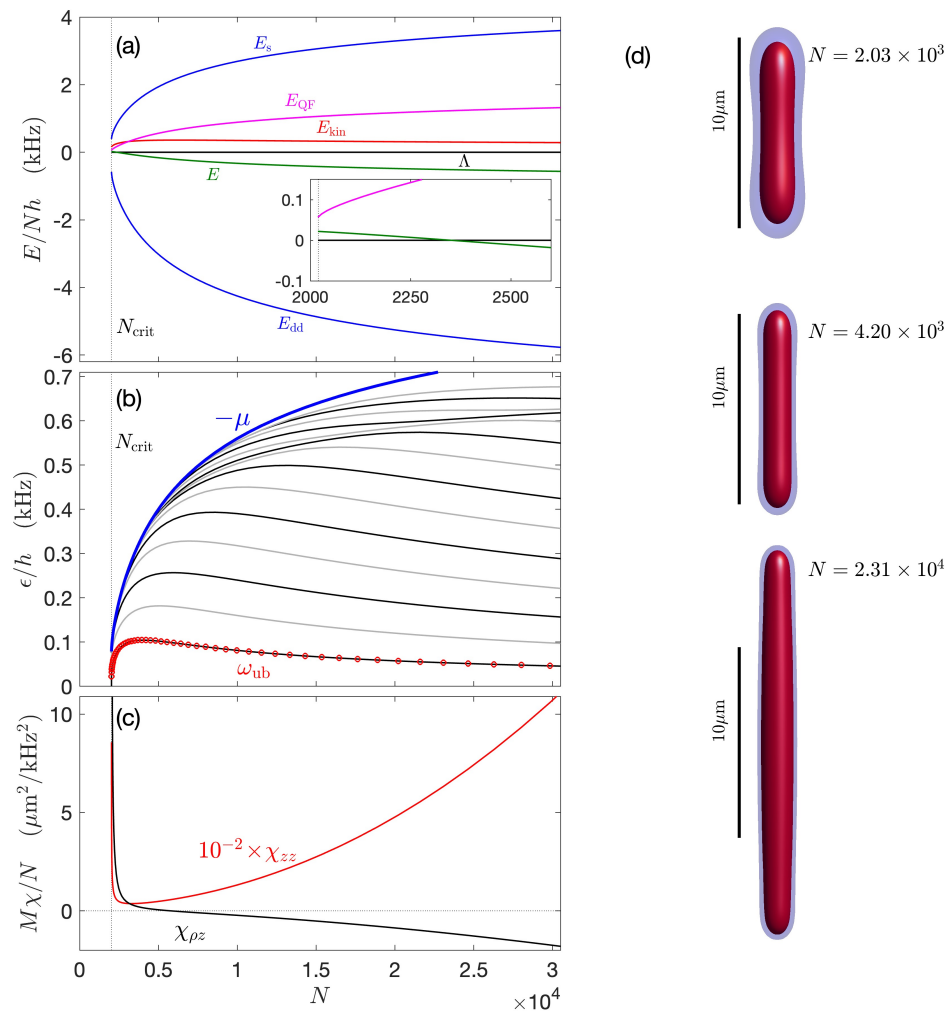


**Figure 1.** Free-space droplet ( $V = 0$ ) as a function of atom number  $N$ . (a) Components of energy and the virial  $\Lambda$ . The inset shows a zoom in close to  $N_{crit} \approx 2020$  to reveal where the total energy is positive. (b) The results from the numerical solution of the BdG equations for the  $m = 0$  excitations that are even (black lines) and odd (grey lines) with respect to a reflection along  $z$  through the droplet center. The approximate result  $\omega_{ub}$  obtained from (15) is shown in red circles. The droplet binding energy, characterized by  $-\mu$ , is shown for reference (blue line). (c) The static polarizabilities  $\chi_{zz}$  and  $\chi_{\rho z}$ . Results are for  $^{164}\text{Dy}$  using  $a_{dd} = 130.8 a_0$  and  $a_s = 80 a_0$ . (d) Density isosurfaces of droplet states for various  $N$  values as labeled. Isosurfaces shown for  $10^{18} \text{ m}^{-3}$  (blue) and  $10^{19} \text{ m}^{-3}$  (red).

### 3.2. Excitations

In Figure 1b we show the spectrum of  $m = 0$  modes in the droplet as a function of  $N$ . Excitations for other  $m$  values were examined in Reference [17]. The lowest energy excitation branch for the quantum droplets is  $m = 0$  (this is not the case for vortex states, e.g., see [27]). We note that the excitations are measured relative to the condensate chemical potential. Thus, excitations with  $\hbar\omega_v > -\mu$  are unbounded by the droplet potential and are thus part of the continuum. For this reason, we only calculate excitations with  $\hbar\omega_v < -\mu$ . From these results we observe that the lowest  $m = 0$  mode becomes soft (i.e., approaches zero energy) as  $N \rightarrow N_{crit}$ . This indicates the onset of a dynamical instability of the self-bound state. We also show the excitation frequency bound  $\omega_{ub}$  obtained from ground state calculations according to Equation (15). This is seen to be in good agreement with the BdG result for the lowest excitation over the full range of atom numbers considered. Indeed, for the results presented,  $\omega_{ub}$  is always greater than the BdG result, with the mean difference being  $\sim 0.8 \text{ Hz}$  (i.e., average relative error of  $\sim 2\%$ ).

In Figure 1c we show the results for the static polarizabilities. The axial result  $\chi_{zz}$  [used in Equation (15)] is always positive, reflecting that the application of a weak axial confinement to the free-space droplet causes it to shorten. The magnitude of  $\chi_{zz}$  tends to be much larger than  $\chi_{\rho z}$ , so we scale it by a factor of  $10^{-2}$  to make the two polarizabilities easier to compare. The transverse response  $\chi_{\rho z}$  changes sign depending on the atom number. In the deeply bound droplet regime (i.e., for  $N > 5 \times 10^3$ , where  $\mu$  is large and negative), it is negative. Thus, a weak compression along  $z$  results in the droplet expanding transversally. In contrast, closer to the unbinding threshold ( $N < 5 \times 10^3$ ),  $\chi_{\rho z}$  is positive, and the transverse width decreases with axial compression. This occurs as the lowest  $m = 0$  mode starts to soften. This change in behavior of the transverse response occurs as the lowest excitation mode changes from quadrupolar character at high  $N$  to monopole (compressional) character at low  $N$  [17].

### 3.3. Results with Varying $a_s$

In Figure 2a we show results for the  $m = 0$  excitations of a free-space droplet with a fixed number  $N = 10^4$ , but with  $a_s$  varying. Here the droplet unbinds at  $a_s \approx 98.5 a_0$ , when the lowest energy mode goes soft. The BdG calculations for the energy of the lowest mode are again seen to be in good agreement with the results of Equation (15). In Figure 2b we examine the response of the ground state to a change in axial confinement. For the deeply bound droplet ( $a_s \lesssim 87 a_0$ )  $\chi_{\rho z}$  is negative, while close to unbinding ( $a_s \gtrsim 87 a_0$ ) it becomes positive [see inset to Figure 2b].

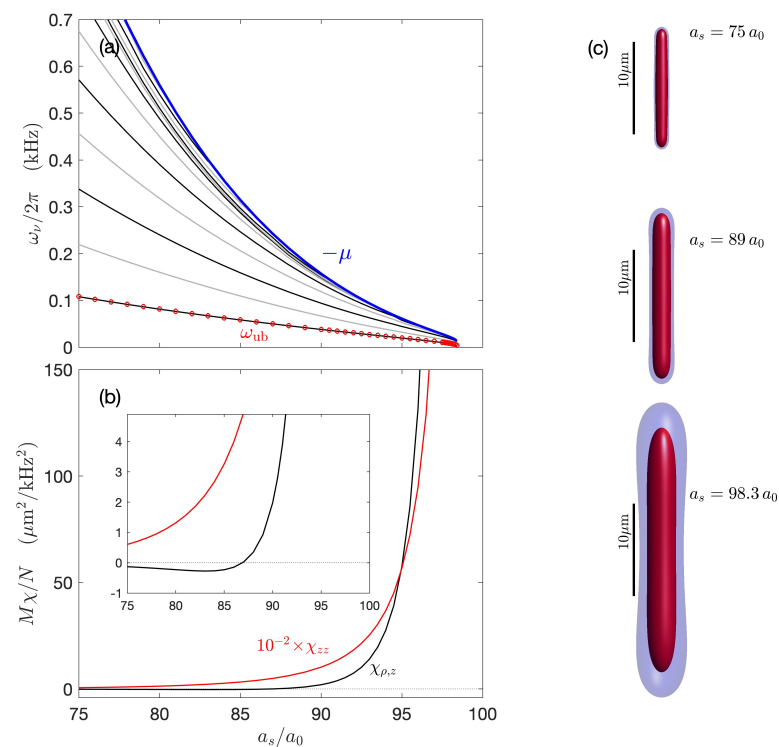


**Figure 2.** Free-space droplet ( $V = 0$ ) as a function of s-wave scattering length  $a_s$ . (a) Results from numerical solution of the BdG equations for the  $m = 0$  excitations that are even (black lines) and odd (grey lines). The droplet binding energy, characterized by  $-\mu$ , is shown for reference (blue line). The approximate result  $\omega_{ub}$  obtained from (15) (red circles). The droplet binding energy, characterized by  $-\mu$ , is shown for reference (blue line). (b) The static polarizabilities  $\chi_{zz}$  and  $\chi_{\rho z}$ . (c) Density isosurfaces of droplet states for various  $a_s$  values as labelled. Isosurfaces shown for  $10^{18} \text{ m}^{-3}$  (blue) and  $10^{19} \text{ m}^{-3}$  (red). Results for  $N = 10^4$   $^{164}\text{Dy}$  atoms using  $a_{dd} = 130.8 a_0$ .

### 4. Results for Trapped Droplet

In Figure 3a we show the excitation spectrum for a droplet confined in a weak cigar-shaped trap  $(\omega_{x,y}, \omega_z) = 2\pi \times (20, 10)$  Hz. This geometry allows a smooth crossover between a self-bound droplet and a trap-bound dipolar BEC. Apart from the trap, the parameters of these results are otherwise identical to the case studied in Figure 2. For  $a_s \lesssim 95 a_0$  the lowest excitation energies, and chemical potential are similar for the trapped and untrapped cases. A notable feature is the emergence of a Kohn mode at the axial trap frequency  $\omega_z$ . The transverse Kohn modes, with frequency  $\omega_{x,y}$ , are in the  $m = \pm 1$  excitation branches and do not appear here. For  $a_s \gtrsim 95 a_0$  the trap starts playing an increasingly important role. In this regime the droplet self-binding begins to fail and the trap provides the confinement [see Figure 3c]. As this happens the chemical potential becomes positive. Since the trap binds excitations at all energy scales, we show BdG results with  $\hbar\omega_\nu > -\mu$ .

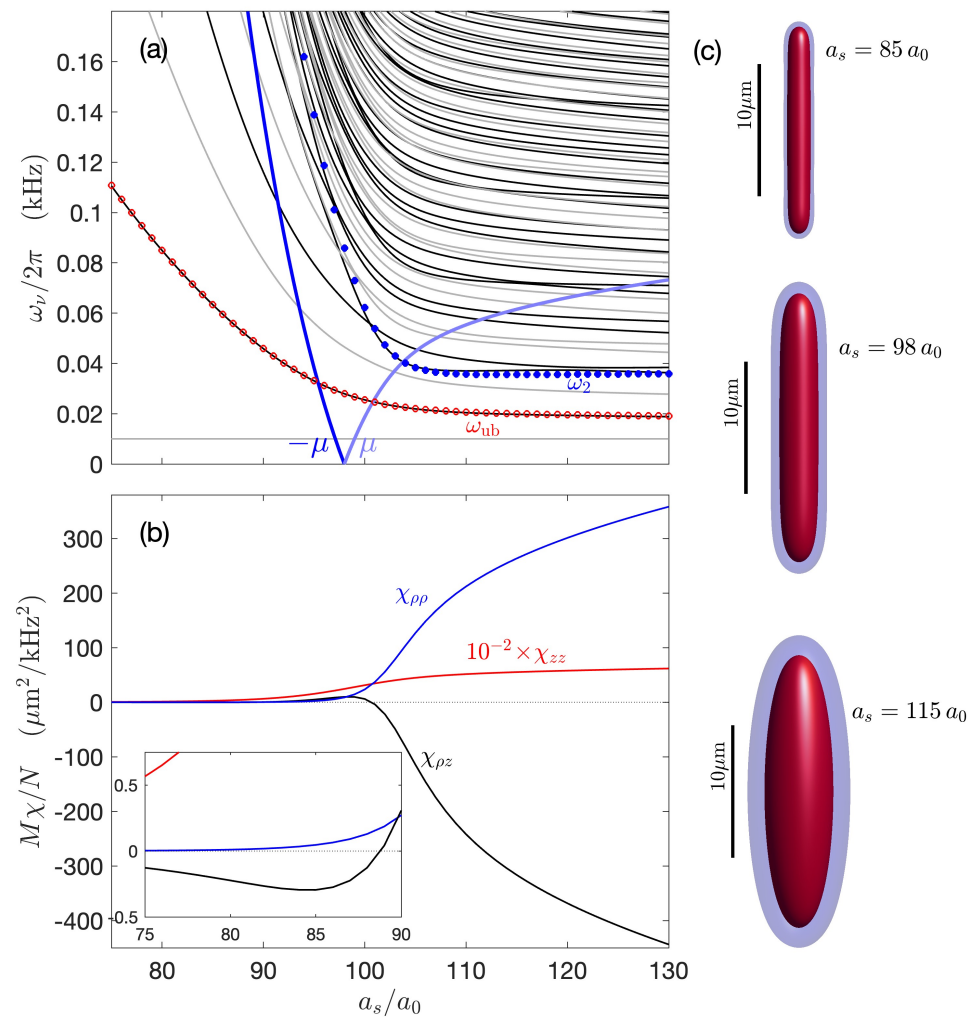


**Figure 3.** Trapped quantum droplet as a function of s-wave scattering length  $a_s$ . (a) Results from numerical solution of the BdG equations for the  $m = 0$  excitations that are even (black lines) and odd (grey lines). The approximate result  $\omega_{ub}$  obtained from (15) (red circles) and the excitation frequency estimate  $\omega_2$  from Equation (23) (blue circles). The energy scales  $\pm\mu$  are shown for reference (blue lines). (b) The static polarizabilities  $\chi_{zz}$ ,  $\chi_{\rho z}$  and  $\chi_{\rho\rho}$ . (c) Density isosurfaces of droplet states for various  $a_s$  values as labelled. Isosurfaces shown for  $10^{18} \text{ m}^{-3}$  (blue) and  $10^{19} \text{ m}^{-3}$  (red). Results for  $N = 10^4$   $^{164}\text{Dy}$  atoms using  $a_{dd} = 130.8 a_0$  and  $(\omega_{x,y}, \omega_z)/2\pi = (20, 10)$  Hz.

For the full range of parameters considered in Figure 3a Equation (15) is seen to provide an accurate description of the axial mode. The lower energy Kohn mode has no effect on

our sum rule since the symmetry of the that mode does not couple to the  $\sigma_z$  operator. In Figure 3a we also present results for the transverse equivalent of Equation (15), i.e.,

$$\omega_2 \equiv \sqrt{\frac{4N\langle\rho^2\rangle}{M\chi_{\rho\rho}}}, \quad (23)$$

where  $\delta\langle\sigma_\rho\rangle = \lambda\chi_{\rho\rho}$  defines the static polarizability for a transverse perturbation of  $-\lambda\sigma_\rho$ . The frequency estimate of Equation (23) is in reasonable agreement with the second even mode in the trap-bound region, but ascends to a high frequency in the droplet regime. These results indicate that Equation (23) is of limited use in the droplet regime.

We show results for the static polarizabilities in Figure 3b. In the droplet regime  $\chi_{zz} \gg |\chi_{\rho\rho}|, |\chi_{\rho z}|$ , while in the trap-bound regime they all become of comparable magnitudes. Interestingly  $\chi_{\rho z}$  is positive at intermediate values of  $a_s$ . Correspondingly we find that the axial mode changes character from being a quadrupolar excitation at low  $a_s$  values, to monopolar at intermediate values, before returning to quadrupolar character at high values of  $a_s$ . Aspects of this behavior has also been described within a variational Gaussian approach [19].

## 5. Conclusions

In this work we presented results for the ground state properties of quantum droplets, their collective excitations and static polarizability related to a change in confinement. We showed that a simple sum rule approach can accurately predict the frequency of the lowest energy (nontrivial) axial collective mode over a wide parameter regime. This mode plays a critical role in the instability of a free-space droplet, and softens to zero energy as the droplet unbinds. Our results for the static polarizabilities quantify changes in the widths of the droplet in response to variations in the axial or transverse confinement. We observed that the transverse static polarizability  $\chi_{\rho z}$  is negative in deeply-bound droplets and is positive for weakly-bound droplets and in the crossover to a trap bound droplet. This change correlates with the lowest excitation changing from having quadrupolar (incompressible) to monopolar (compressible) character.

The lowest energy axial collective mode was measured in experiments by Chomaz et al. [16] for a dipolar BEC under confinement in the crossover regime to a quantum droplet. Our results motivate further experiments to study this collective excitation, ideally for a system with lower loss where it will be possible to study this excitation in more deeply bound droplets. It would also be interesting to quantify the static response of the droplet. Since the  $\chi_{\rho z}$  and  $\chi_{\rho\rho}$  responses are typically much smaller than  $\chi_{zz}$  in the droplet regime, and may be challenging to measure these with optical imaging.

**Funding:** This research was funded by the Marsden Fund of the Royal Society of New Zealand.

**Institutional Review Board Statement:** Not applicable.

**Informed Consent Statement:** Not applicable.

**Data Availability Statement:** Data available on request.

**Acknowledgments:** PBB wishes to acknowledge use of the New Zealand eScience Infrastructure (NeSI) high performance computing facilities. Helpful discussions with D. Baillie, A.-C. Lee and J. Smith are acknowledged.

**Conflicts of Interest:** The author declares no conflict of interest.

## References

1. Griesmaier, A.; Werner, J.; Hensler, S.; Stuhler, J.; Pfau, T. Bose-Einstein Condensation of Chromium. *Phys. Rev. Lett.* **2005**, *94*, 160401. [[CrossRef](#)] [[PubMed](#)]
2. Beaufils, Q.; Chicireanu, R.; Zanon, T.; Laburthe-Tolra, B.; Maréchal, E.; Vernac, L.; Keller, J.C.; Gorceix, O. All-optical production of chromium Bose-Einstein condensates. *Phys. Rev. A* **2008**, *77*, 061601. [[CrossRef](#)]

3. Lu, M.; Burdick, N.Q.; Youn, S.H.; Lev, B.L. Strongly Dipolar Bose-Einstein Condensate of Dysprosium. *Phys. Rev. Lett.* **2011**, *107*, 190401. [[CrossRef](#)]
4. Aikawa, K.; Frisch, A.; Mark, M.; Baier, S.; Rietzler, A.; Grimm, R.; Ferlaino, F. Bose-Einstein Condensation of Erbium. *Phys. Rev. Lett.* **2012**, *108*, 210401. [[CrossRef](#)] [[PubMed](#)]
5. Lahaye, T.; Menotti, C.; Santos, L.; Lewenstein, M.; Pfau, T. The physics of dipolar bosonic quantum gases. *Rep. Prog. Phys.* **2009**, *72*, 126401. [[CrossRef](#)]
6. Chomaz, L.; Ferrier-Barbut, I.; Ferlaino, F.; Laburthe-Tolra, B.; Lev, B.L.; Pfau, T. Dipolar physics: A review of experiments with magnetic quantum gases. *Rep. Prog. Phys.* **2022**, *86*, 026401. [[CrossRef](#)]
7. Lee, T.D.; Huang, K.; Yang, C.N. Eigenvalues and Eigenfunctions of a Bose System of Hard Spheres and Its Low-Temperature Properties. *Phys. Rev.* **1957**, *106*, 1135–1145. [[CrossRef](#)]
8. Lima, A.R.P.; Pelster, A. Quantum fluctuations in dipolar Bose gases. *Phys. Rev. A* **2011**, *84*, 041604. [[CrossRef](#)]
9. Lima, A.R.P.; Pelster, A. Beyond mean-field low-lying excitations of dipolar Bose gases. *Phys. Rev. A* **2012**, *86*, 063609. [[CrossRef](#)]
10. Petrov, D.S. Quantum Mechanical Stabilization of a Collapsing Bose-Bose Mixture. *Phys. Rev. Lett.* **2015**, *115*, 155302. [[CrossRef](#)]
11. Ferrier-Barbut, I.; Kadau, H.; Schmitt, M.; Wenzel, M.; Pfau, T. Observation of Quantum Droplets in a Strongly Dipolar Bose Gas. *Phys. Rev. Lett.* **2016**, *116*, 215301. [[CrossRef](#)]
12. Wächtler, F.; Santos, L. Quantum filaments in dipolar Bose-Einstein condensates. *Phys. Rev. A* **2016**, *93*, 061603(R). [[CrossRef](#)]
13. Bisset, R.N.; Wilson, R.M.; Baillie, D.; Blakie, P.B. Ground-state phase diagram of a dipolar condensate with quantum fluctuations. *Phys. Rev. A* **2016**, *94*, 033619. [[CrossRef](#)]
14. Kadau, H.; Schmitt, M.; Wenzel, M.; Wink, C.; Maier, T.; Ferrier-Barbut, I.; Pfau, T. Observing the Rosensweig instability of a quantum ferrofluid. *Nature* **2016**, *530*, 194–197. [[CrossRef](#)]
15. Schmitt, M.; Wenzel, M.; Böttcher, F.; Ferrier-Barbut, I.; Pfau, T. Self-bound droplets of a dilute magnetic quantum liquid. *Nature* **2016**, *539*, 259–262. [[CrossRef](#)]
16. Chomaz, L.; Baier, S.; Petter, D.; Mark, M.J.; Wächtler, F.; Santos, L.; Ferlaino, F. Quantum-Fluctuation-Driven Crossover from a Dilute Bose-Einstein Condensate to a Macrodroplet in a Dipolar Quantum Fluid. *Phys. Rev. X* **2016**, *6*, 041039. [[CrossRef](#)]
17. Baillie, D.; Wilson, R.M.; Blakie, P.B. Collective Excitations of Self-Bound Droplets of a Dipolar Quantum Fluid. *Phys. Rev. Lett.* **2017**, *119*, 255302. [[CrossRef](#)]
18. Pal, S.; Baillie, D.; Blakie, P.B. Infinite dipolar droplet: A simple theory for the macrodroplet regime. *Phys. Rev. A* **2022**, *105*, 023308. [[CrossRef](#)]
19. Wächtler, F.; Santos, L. Ground-state properties and elementary excitations of quantum droplets in dipolar Bose-Einstein condensates. *Phys. Rev. A* **2016**, *94*, 043618. [[CrossRef](#)]
20. Ferrier-Barbut, I.; Wenzel, M.; Böttcher, F.; Langen, T.; Isoard, M.; Stringari, S.; Pfau, T. Scissors Mode of Dipolar Quantum Droplets of Dysprosium Atoms. *Phys. Rev. Lett.* **2018**, *120*, 160402. [[CrossRef](#)] [[PubMed](#)]
21. Lee, A.C.; Baillie, D.; Blakie, P.B. Numerical calculation of dipolar-quantum-droplet stationary states. *Phys. Rev. Res.* **2021**, *3*, 013283. [[CrossRef](#)]
22. Pitaevskii, L.; Stringari, S. *Bose-Einstein Condensation and Superfluidity*; Oxford University Press: Oxford, UK, 2016; Volume 164,
23. Menotti, C.; Stringari, S. Collective oscillations of a one-dimensional trapped Bose-Einstein gas. *Phys. Rev. A* **2002**, *66*, 043610. [[CrossRef](#)]
24. Tanzi, L.; Rocuzzo, S.M.; Lucioni, E.; Famà, F.; Fioretti, A.; Gabbanini, C.; Modugno, G.; Recati, A.; Stringari, S. Supersolid symmetry breaking from compressional oscillations in a dipolar quantum gas. *Nature* **2019**, *574*, 382. [[CrossRef](#)] [[PubMed](#)]
25. Dalfovo, F.; Giorgini, S.; Pitaevskii, L.; Stringari, S. Theory of Bose-Einstein condensation in trapped gases. *Rev. Mod. Phys.* **1999**, *71*, 463. [[CrossRef](#)]
26. Triay, A. Existence of minimizers in generalized Gross-Pitaevskii theory with the Lee-Huang-Yang correction. *arXiv* **2019**, arXiv:1904.10672.
27. Lee, A.C.; Baillie, D.; Bisset, R.N.; Blakie, P.B. Excitations of a vortex line in an elongated dipolar condensate. *Phys. Rev. A* **2018**, *98*, 063620. [[CrossRef](#)]

**Disclaimer/Publisher's Note:** The statements, opinions and data contained in all publications are solely those of the individual author(s) and contributor(s) and not of MDPI and/or the editor(s). MDPI and/or the editor(s) disclaim responsibility for any injury to people or property resulting from any ideas, methods, instructions or products referred to in the content.